Supporting Information

Chromous siloxides of variable nuclearity and magnetism

Simon P. O. Trzmiel,[a] Jan Langmann,[b] Cäcilia Maichle-Mössmer,[a] and Reiner Anwander[a],*

a) Institut für Anorganische Chemie, Eberhard Karls Universität Tübingen, Auf der Morgenstelle 18, 72076 Tübingen, Germany

b) Institut für Physik, Universität Augsburg, Universitätsstr. 1, 86159 Augsburg, Germany

*E-mail for R. A.: reiner.anwander@uni-tuebingen.de

## Table of Contents

Magnetic Measurements
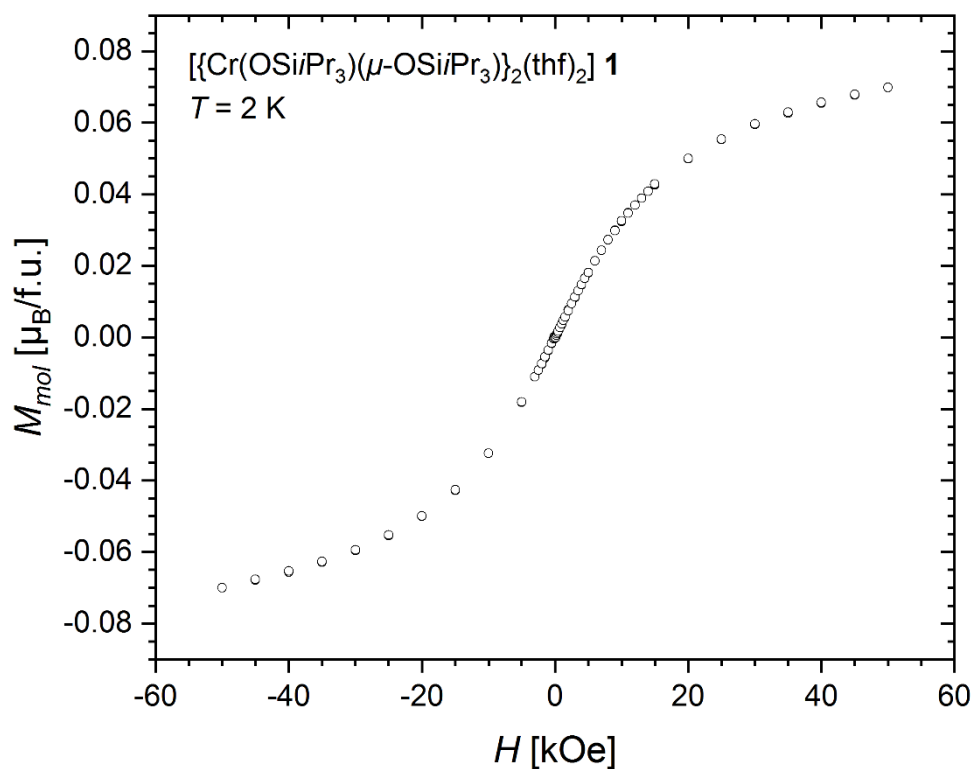
Figure S1. Field-dependent molar magnetization $M_{mol}(H)$ (black open circles) as obtained by SQUID magnetic measurements on crystalline powder of **1** at a temperature $T = 2$ K.
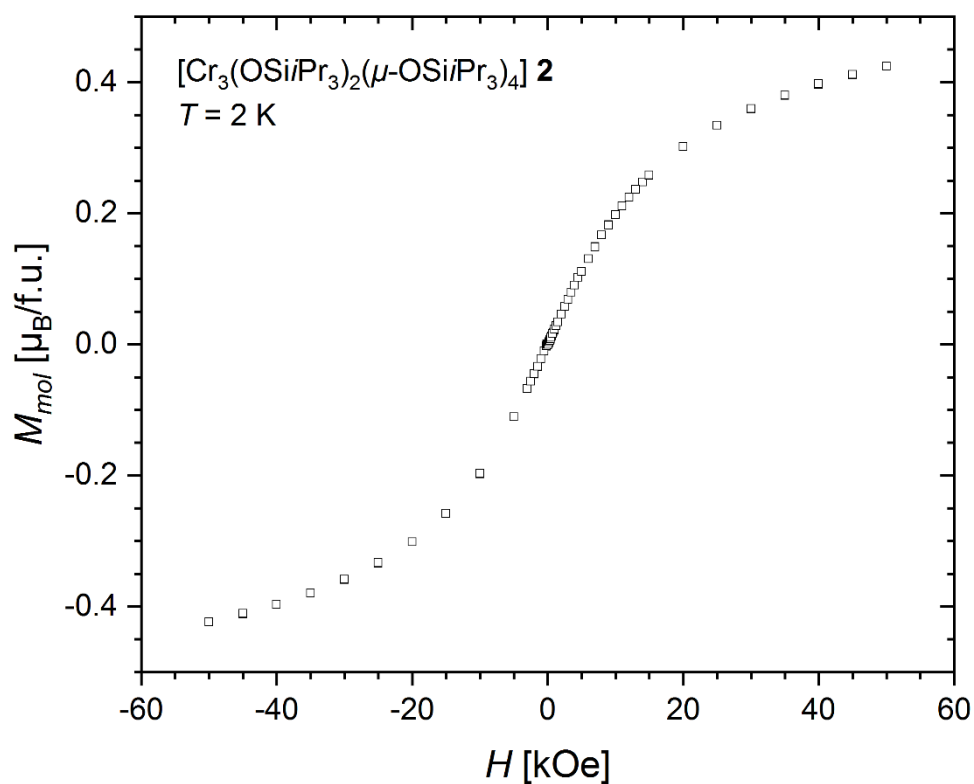
Figure S2. Field-dependent molar magnetization $M_{mol}(H)$ (black open circles) as obtained by SQUID magnetic measurements on crystalline powder of **2** at a temperature $T = 2$ K.
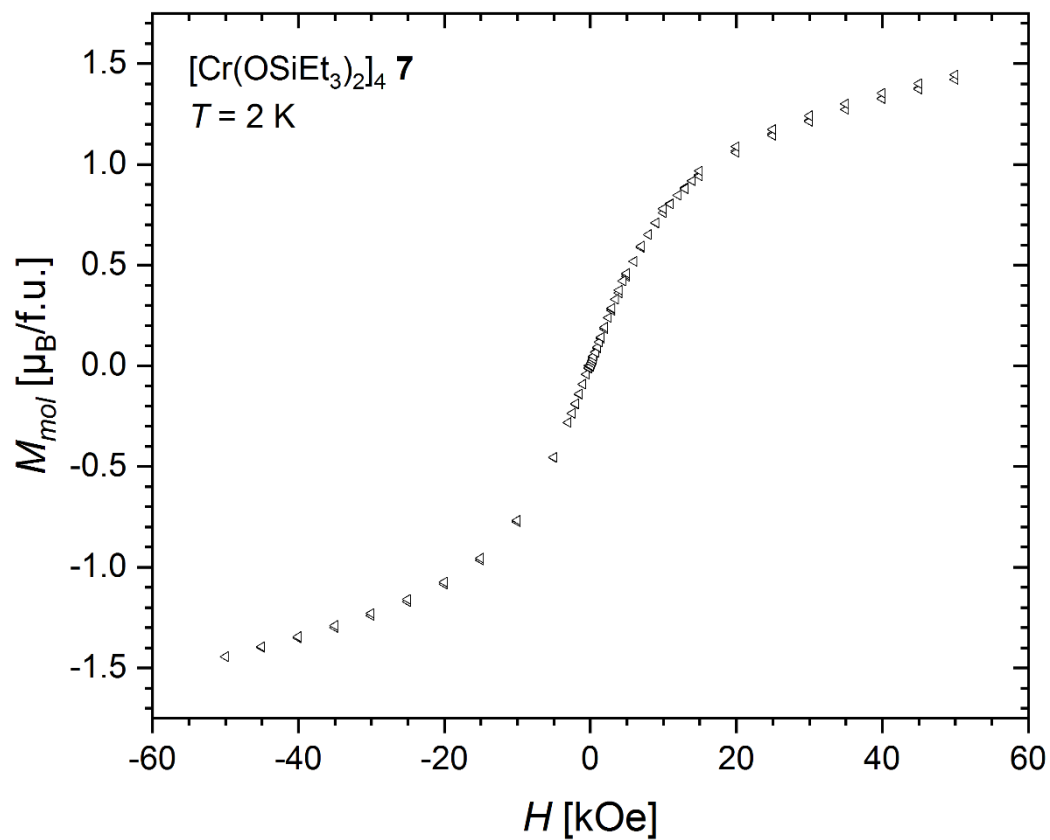
Figure S3. Field-dependent molar magnetization $M_{mol}(H)$ (black open circles) as obtained by SQUID magnetic measurements on crystalline powder of **7** at a temperature $T = 2$ K.

NMR Spectra
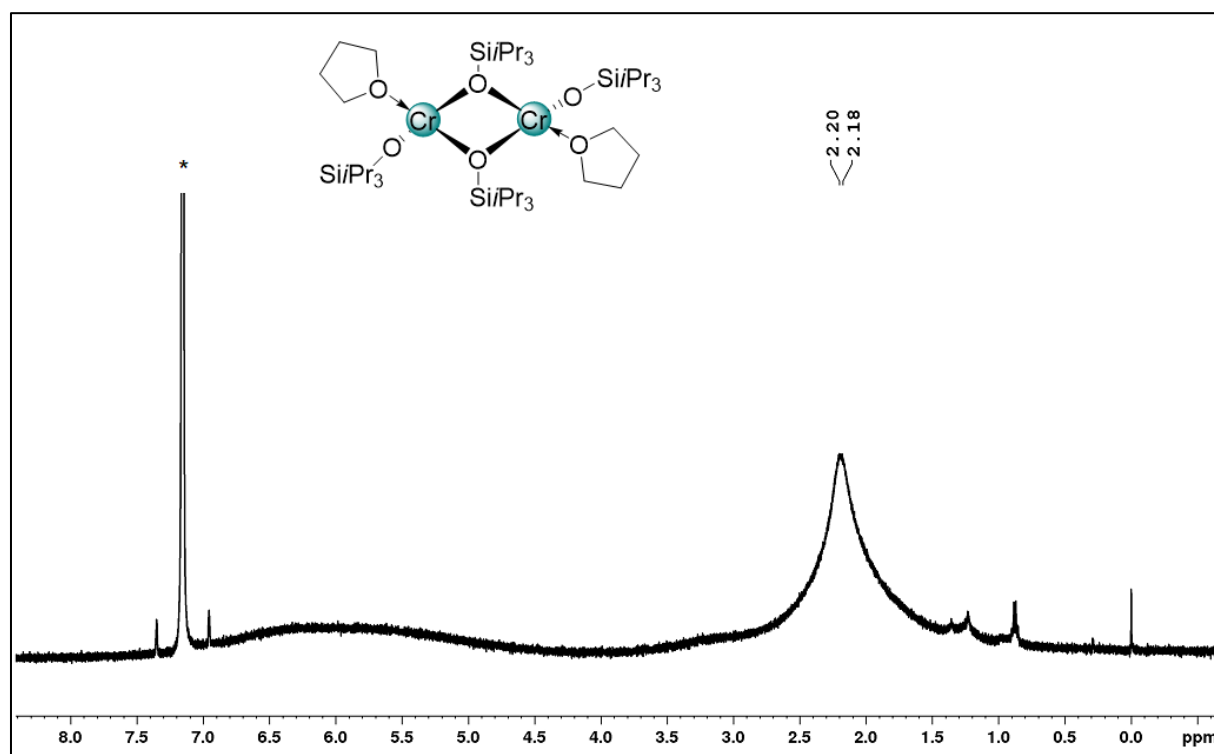
Figure S4. ^{1}H NMR spectrum (26 °C, 400.13 MHz, benzene-d6) of Cr2(OSi*i*Pr3)2(μ-OSi*i*Pr3)2(thf)2 (**1**).
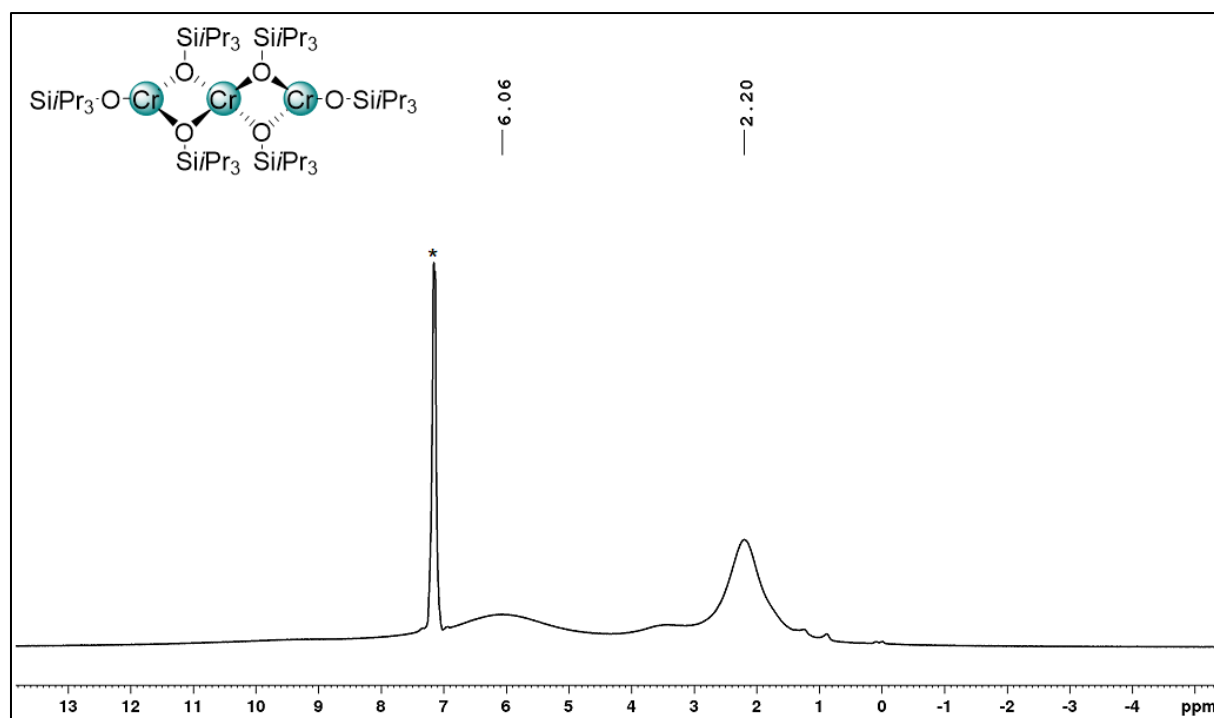
Figure S5. ^{1}H NMR spectrum (26 °C, 400.13 MHz, benzene-d6) of Cr3(OSi*i*Pr3)2(μ-OSi*i*Pr3)4 (**2**).
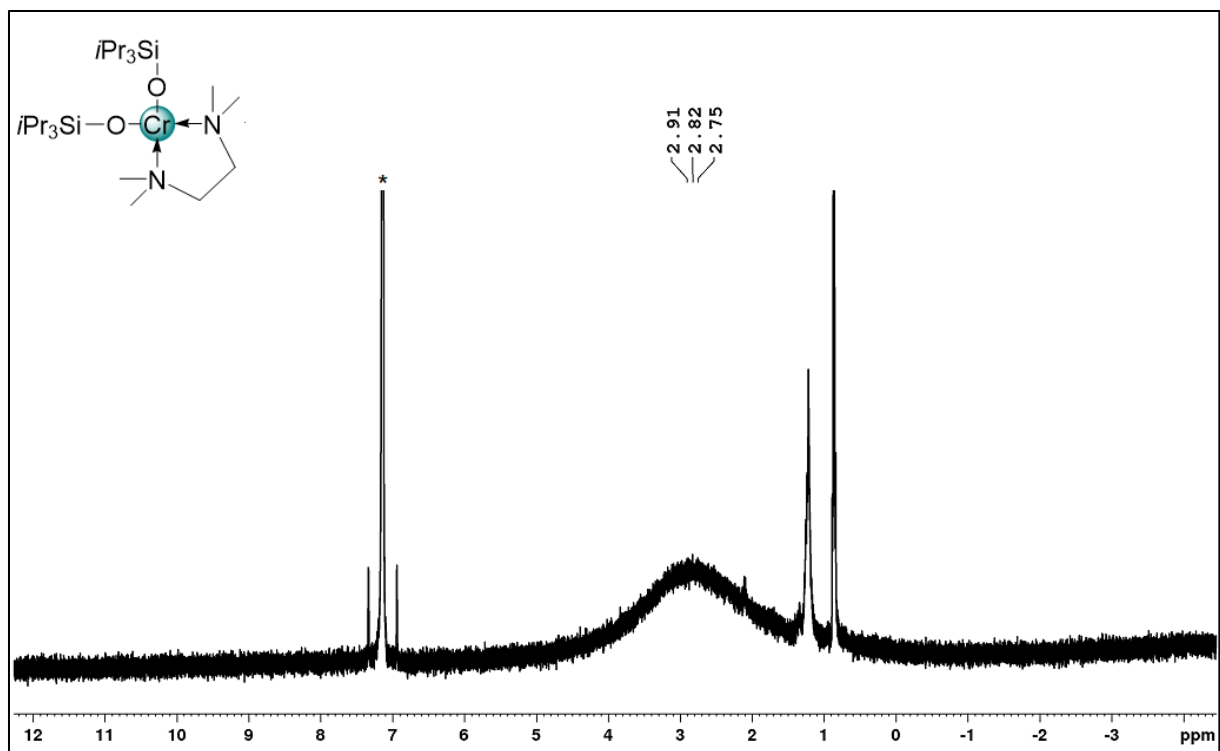
Figure S6. ^{1}H NMR spectrum (26 °C, 400.13 MHz, benzene-d_6) of Cr(OSiiPr$_3$)$_2$(tmeda) (**3**).
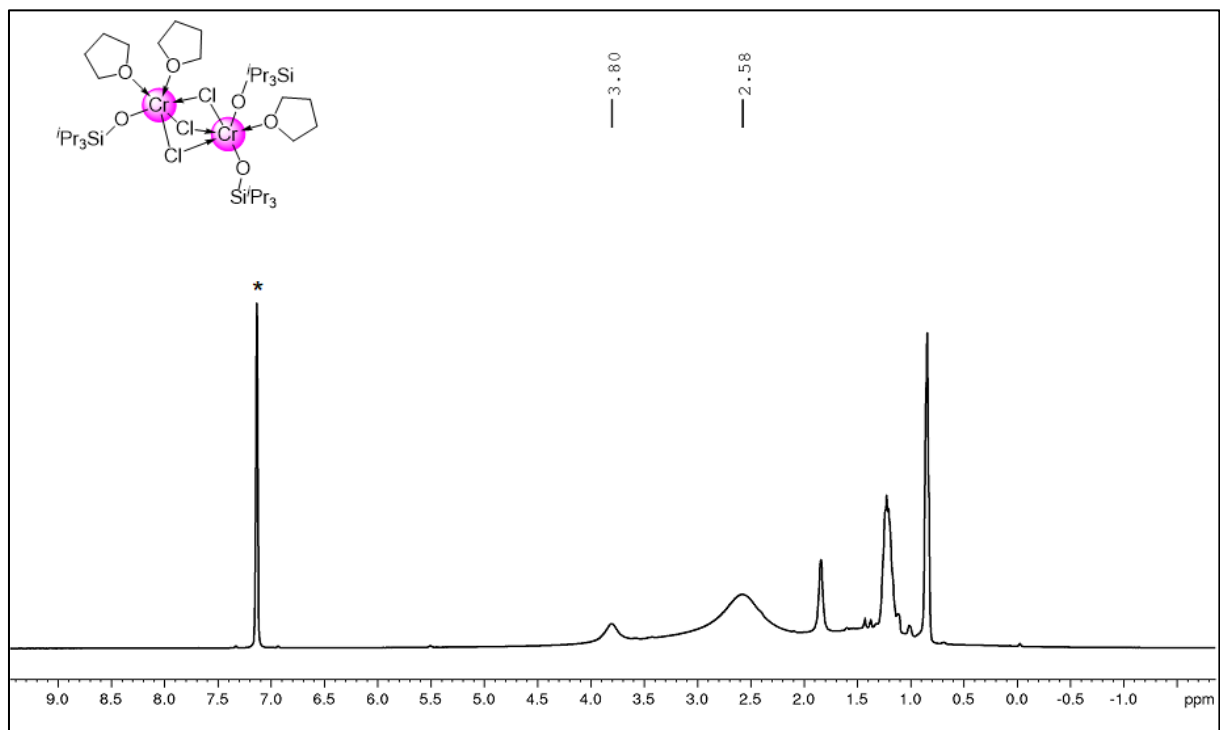
Figure S7. ^{1}H NMR spectrum (26 °C, 400.13 MHz, benzene-d_6) of Cr$_2$Cl$_3$(OSiiPr$_3$)$_3$(thf)$_3$ (**5**).
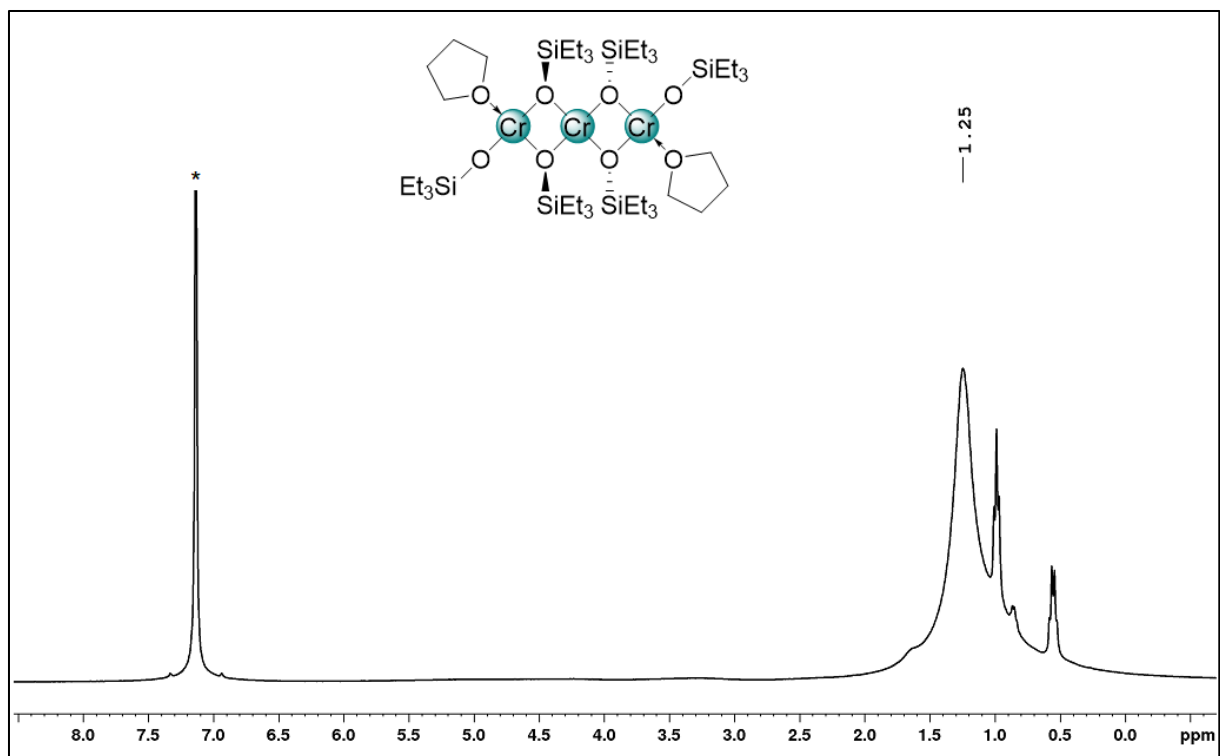
Figure S8. ^{1}H NMR spectrum (26 °C, 400.13 MHz, benzene-d_6) of $Cr_3(OSiEt_3)_2(\mu\text{-}OSi\textit{i}Et_3)_4(thf)_2$ (**6**).
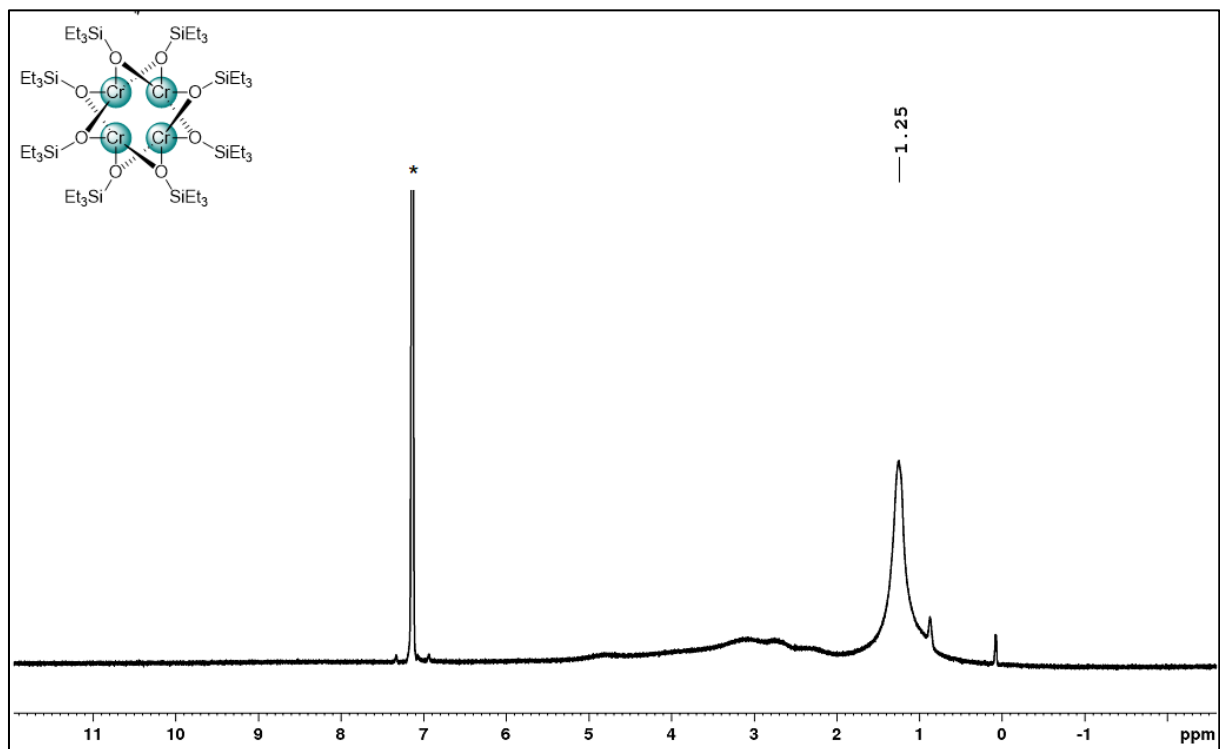
**Figure S9.** ^{1}H NMR spectrum (26 °C, 400.13 MHz, benzene-d_6) of $Cr_4(OSiEt_3)_8$ (**7**).

IR Spectra
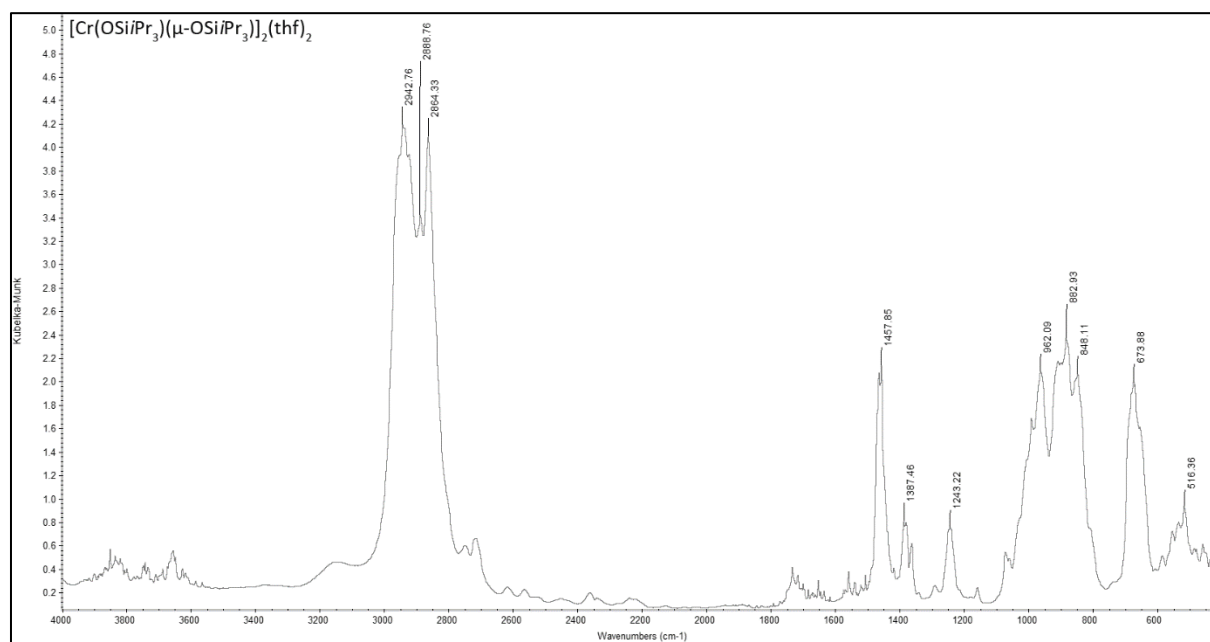
Figure S10. DRIFT spectrum of compound **1** measured on KBr.
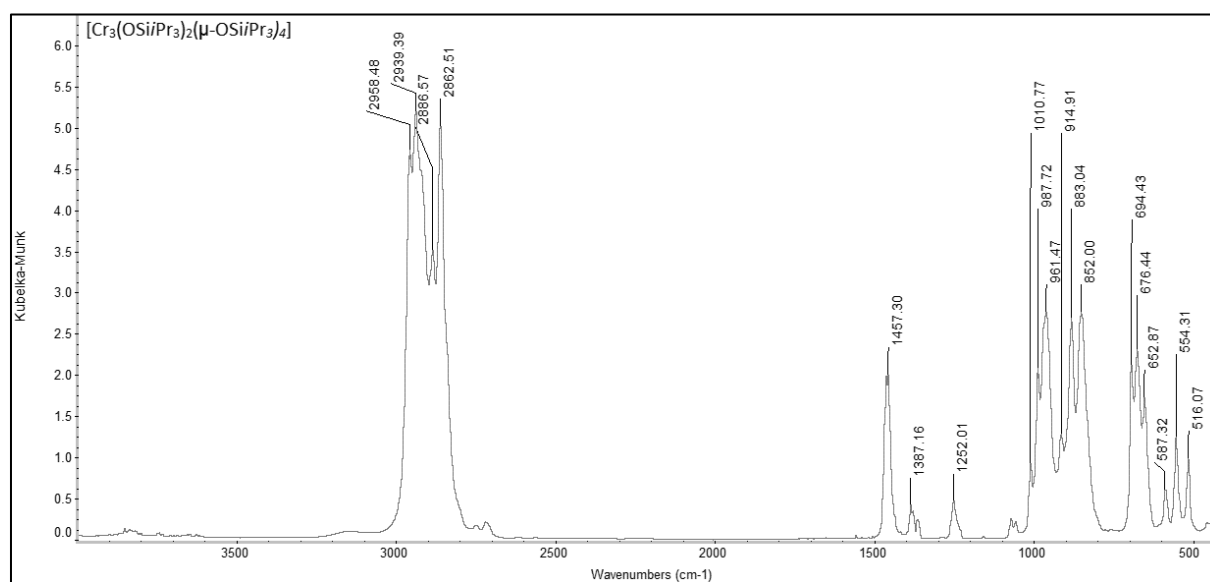
Figure S11. DRIFT spectrum of compound **2** measured on KBr.
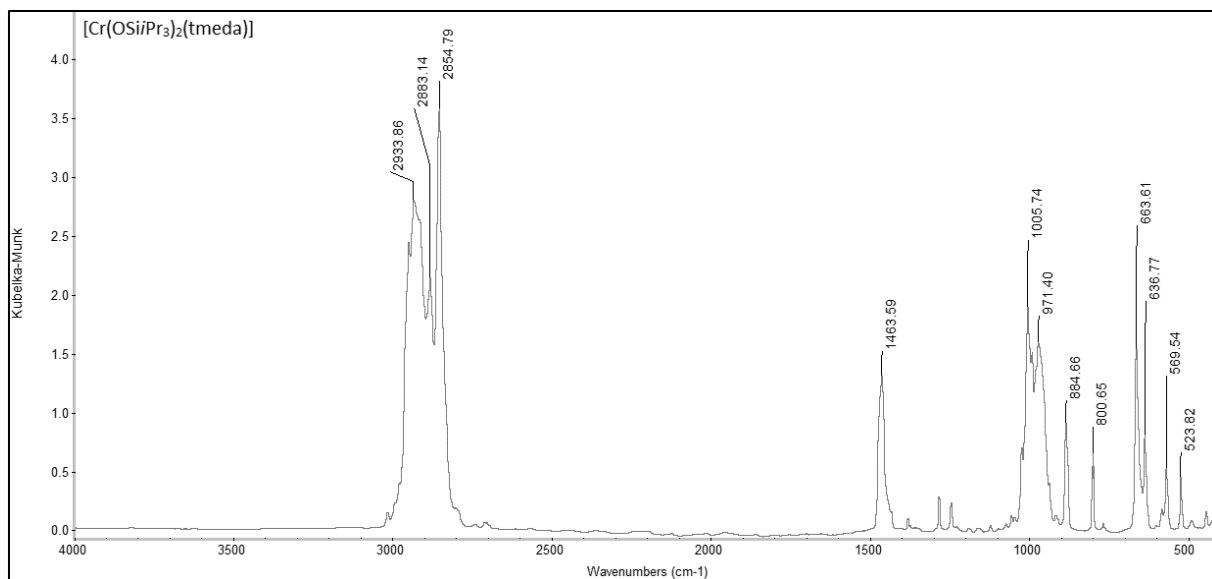
Figure S12. DRIFT spectrum of compound **3** measured on KBr.
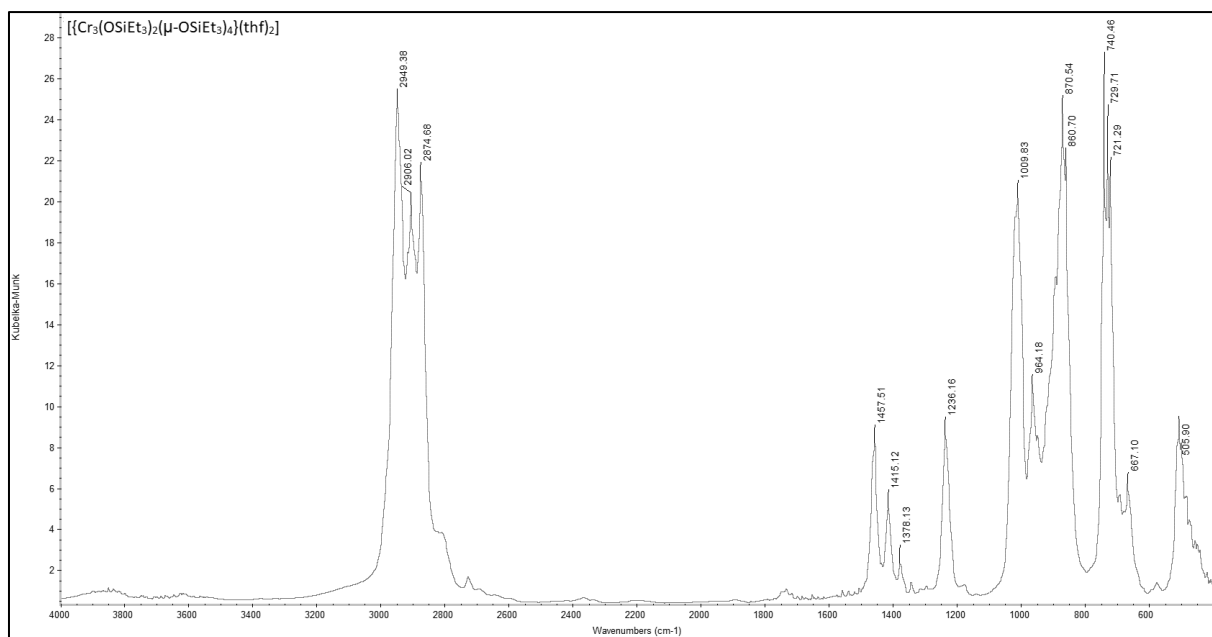
Figure S13. DRIFT spectrum of compound **6** measured on KBr.
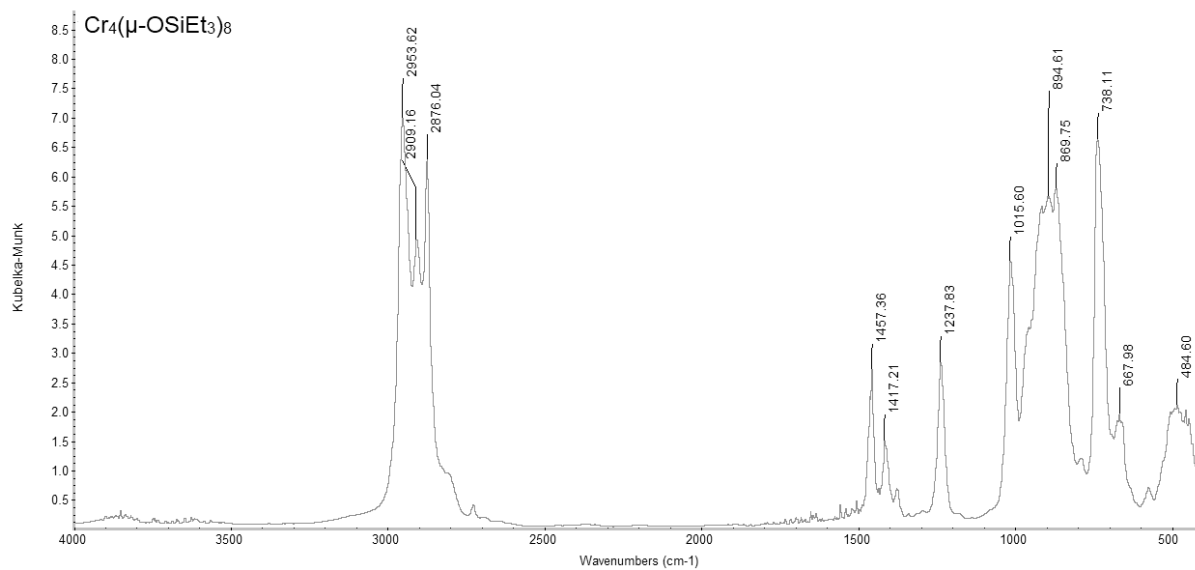
Figure S14. DRIFT spectrum of compound **7** measured on KBr.
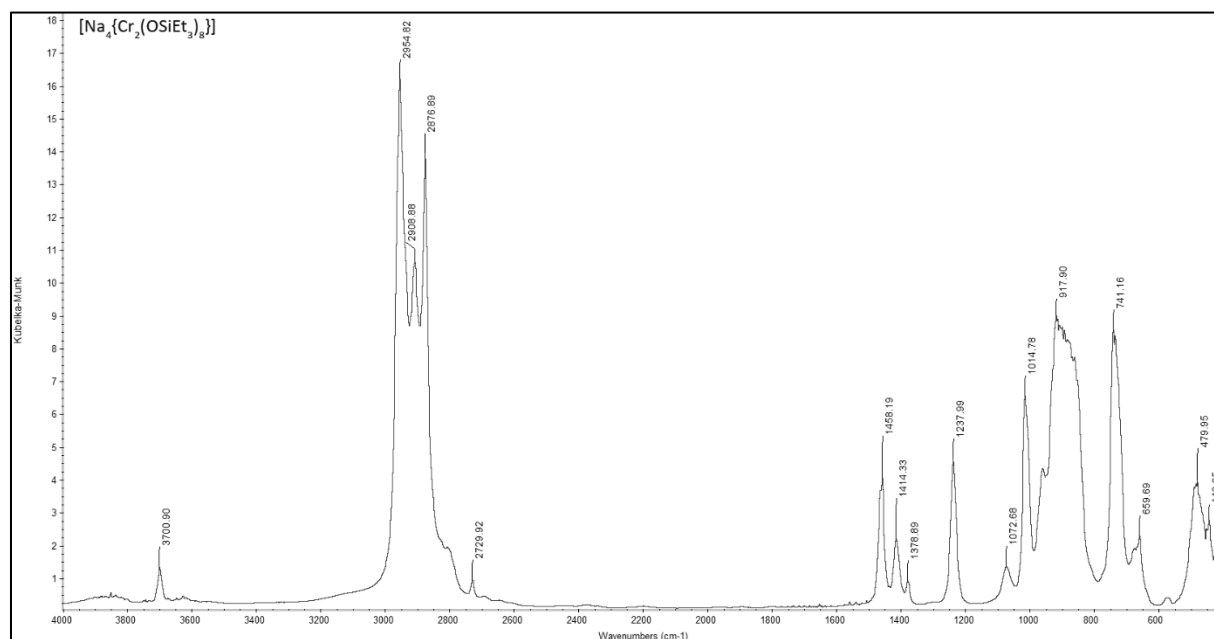
Figure S15. DRIFT spectrum of compound **8** measured on KBr.

UV-vis Spectra

$[Cr(OSiiPr_3)(\mu\text{-}OSiiPr_3)(thf)]_2$
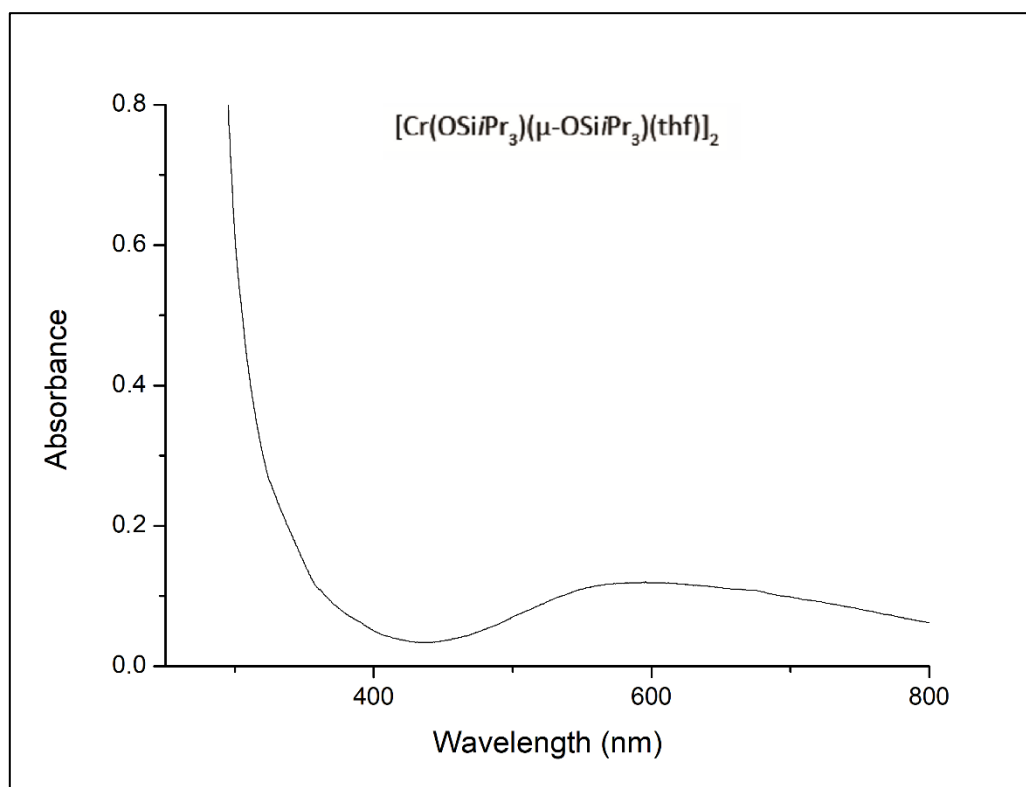
Figure S16. UV-vis spectrum of compound **1** in dilute *n*-hexane solution (concentration c = 4.9*10⁻⁶ [mol*L⁻¹], ε_{590}= 2.4*10⁴ L*mol⁻¹*cm⁻¹).

$[Cr_3(OSiiPr_3)_2(\mu\text{-}OSiiPr_3)_4]$
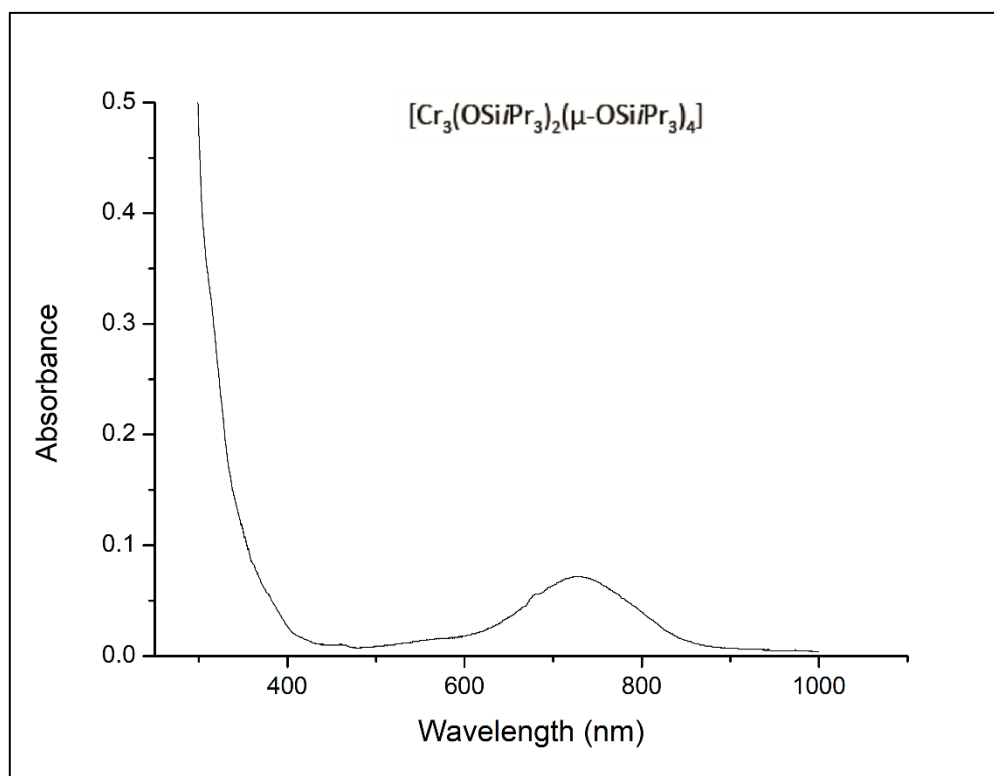
Figure S17. UV-vis spectrum of compound **2** in dilute *n*-hexane solution (c = 3.9*10⁻⁶ [mol*L⁻¹], ε_{727}= 1.8*10⁴ L*mol⁻¹*cm⁻¹).
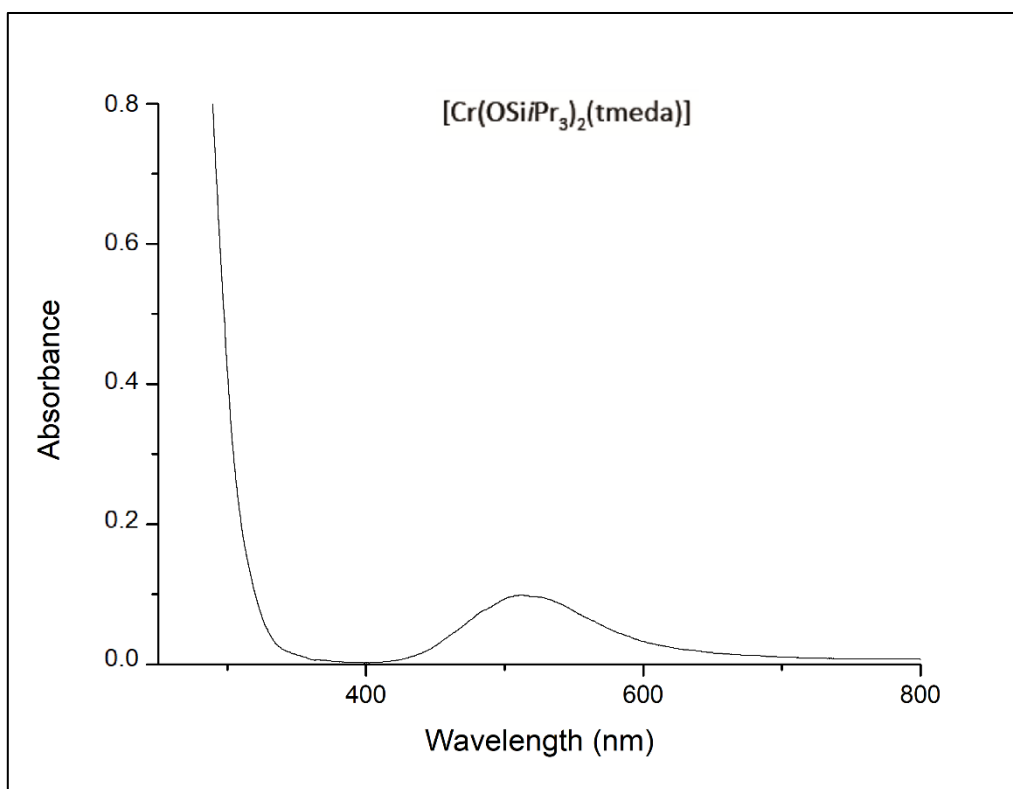
Figure S18. UV-vis spectrum of compound **3** in dilute *n*-hexane solution (concentration c = 2.2*10^{-5} [mol*L^{-1}], ε_{508}= 4.3*10^4 L*mol^{-1}*cm^{-1}).
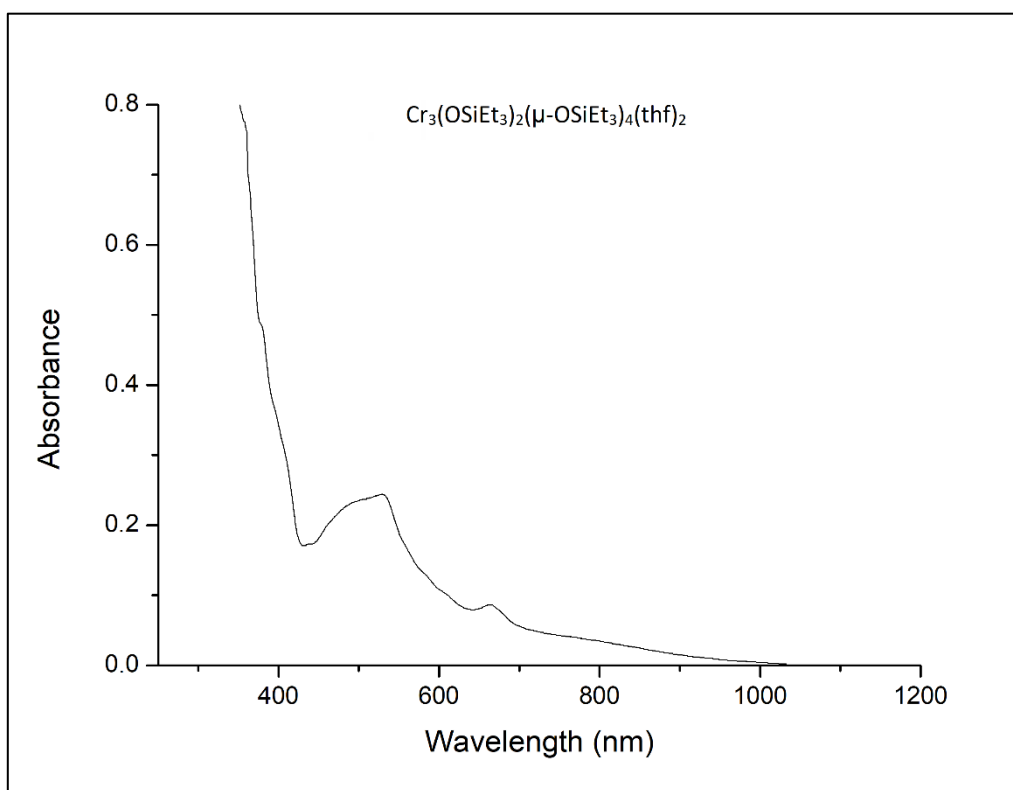
Figure S19. UV-vis spectrum of compound **6** in dilute *n*-hexane solution (concentration c = 1.1*10^{-5} [mol*L^{-1}], ε_{528}= 2.2*10^4 L*mol^{-1}*cm^{-1}).
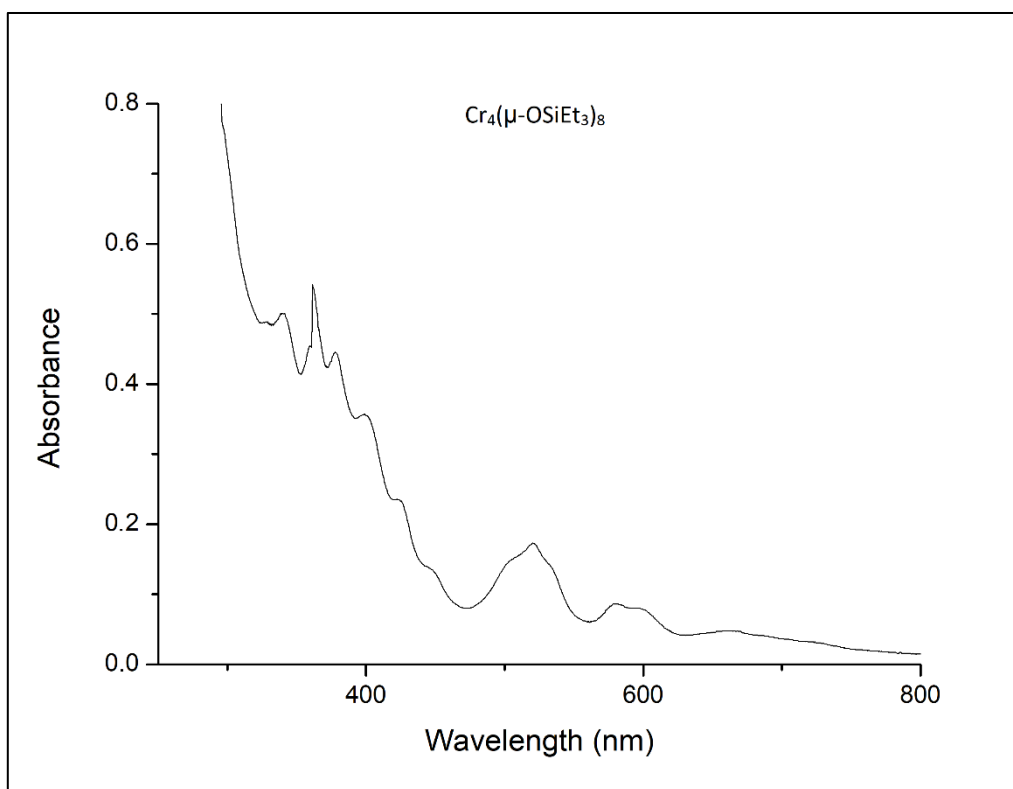
Figure S20. UV-vis spectrum of compound **7** in dilute *n*-hexane solution (concentration c = 6.2*10^{-6} [mol*L^{-1}], ε_{520}= 2.7*10^4 ε_{361}= 8.7*10^4 L*mol^{-1}*cm^{-1}).
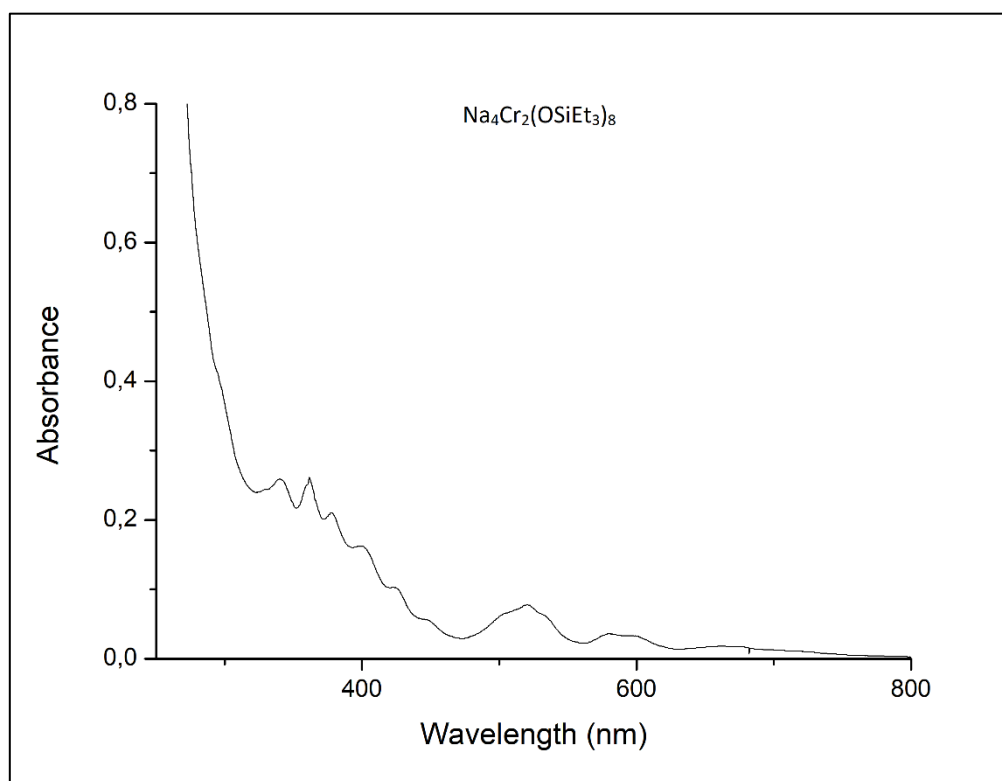
Figure S21. UV-vis spectrum of compound **8** in dilute *n*-hexane solution.

# Crystallographic Information

Table S1. Crystallographic data for compound **1**, **2**, **3**, **4** and, **5**

	[Cr(OSi*i*Pr₃)(μ-OSi*i*Pr₃)(thf)]₂ (**1**)	[Cr₃(OSi*i*Pr₃)₂(μ-OSi*i*Pr₃)₄] (**2**)	[Cr(OSi*i*Pr₃)₂(tmeda)] (**3**)	[Cr(OSi*i*Pr₃)₃(thf)₂] (**4**)	[Cr₂Cl₃(OSi*i*Pr₃)₃(thf)₃] (**5**)
Formula	$C_{44}H_{100}Cr_2O_6Si_4$	$C_{54}H_{126}Cr_3O_6Si_6$	$C_{24}H_{58}CrN_2O_2Si_2$	$C_{35}H_{79}CrO_5Si_3$	$C_{39}H_{87}Cl_3Cr_2O_6Si_3$
CCDC	2149139	2149143	2149140	2149142	2149145
M_r [g mol⁻¹]	941.59	1196.08	514.90	716.25	946.70
color	violet/blocks			violet/block	violet plates
crystal system	Monoclinic	Triclinic	Monoclinic	Orthorhombic	Monoclinic
space group	C 2/c	$P\bar{1}$	P2₁/c	P n a 21	P2₁/c
a [Å]	26.0872(13)	13.8340(8)	20.997(4)	45.286(4)	12.7399(15)
b [Å]	11.7092(6)	14.4338(9)	29.553(5)	13.8630(12)	20.409(2)
c [Å]	21.6971(11)	18.5308(11)	15.170(3)	13.4511(11)	20.149(2)
α [°]	90	104.537(2)	90	90	90
β [°]	123.1860(10)	100.026(2)	102.489(2)	90	104.579(2)
γ [°]	90	95.480(2)	90	90	90
V [Å³]	5546.6(5)	3489.2(4)	9191(3)	8444.6(12)	5070.1(10)
Z	4	2	12	8	4
T [K]	100(2)	173(2)	173(2)	100(2)	100(2)
ρ_{calcd} [g cm⁻³]	1.128	1.138	1.116	1.127	1.240
μ [mm⁻¹]	0.517	0.602	0.472	0.391	0.696
F (000)	2064	1308	3408	3160	2040
total reflns	40844	113301	167843	61112	101344
observed reflns (I>2σ)	5008	10791	16855	17260	11698
R_1/wR_2 (I > 2σ)[a]	0.0377/ 0.0882	0.0453/ 0.1093	0.0463/ 0.1224	0.0421/ 0.0994	0.0271/ 0.0690
R_1/wR_2 (all data)[a]	0.0557/ 0.0989	0.0594/0.1228	0.0817/ 0.1479	0.0540/ 0.1064	0.0321/ 0.0726
GOF	1.035	1.035	1.015	1.030	1.026

[a] $R1 = \Sigma(||F_0|-|F_c||)/\Sigma|F_0|, F_0 > 4s(F_0)$. $\omega R2 = \{\Sigma[\omega\,(F_0^2-F_c^2)^2/\Sigma[\omega\,(F_0^2)^2]\}^{1/2}$.

Table S2. Crystallographic data for compounds **6**, **7** and **8**

	[Cr₃(OSiEt₃)₂(μ-OSiEt₃)₄(thf)₂] (**6**)	[Cr(OSiEt₃)₂]₄ (**7**)	[Na₄Cr₂(OSiEt₃)₈] (**8**)
Formula	$C_{44}H_{106}Cr_3O_8Si_6$	$C_{48}H_{120}Cr_4O_8Si_8$	$C_{48}H_{120}Cr_{2.20}Na_{3.80}O_8Si_8$
CCDC	2149144	2149141	2149146
M_r [g mol⁻¹]	1087.82	1258.15	1252.01
color	red/blocks	brown/ blocks	brown/ blocks
crystal system	Triclinic	Monoclinic	Trigonal
space group	$P\bar{1}$	C2/c	R3c
a [Å]	11.4293(5)	25.353(3)	14.251(3)
b [Å]	12.4998(6)	12.0914(15)	14.251(3)
c [Å]	12.9835(6)	24.967(3)	59.481(12)
α [°]	62.2170(10)	90	90.00(3)
β [°]	67.7320(10)	116.114(2)	90.00(3)
γ [°]	89.9490(10)	90	120.00(3)
V [Å³]	1483.26(12)	6872.5(15)	10462(5)
Z	1	4	6
T [K]	100(2)	100(2)	99(2)
ρ_{calcd} [g cm⁻³]	1.218	1.216	1.192
μ [mm⁻¹]	0.703	0.797	0.544
F (000)	590	2720	4072
total reflns	54868	48774	60582
observed reflns (I>2σ)	6198	5628	6074
R_1/wR_2 (I > 2σ)[a]	0.0297/0.0756	0.0432/ 0.0948	0.0382/ 0.0994
R_1/wR_2 (all data)[a]	0.0357/0.0797	0.0685/ 0.1076	0.0463/ 0.1085
GOF	1.084	1.028	1.036

[a] $R1 = \Sigma(||F_0|-|F_c||)/\Sigma|F_0|, F_0 > 4s(F_0)$. $\omega R2 = \{\Sigma[\omega\ (F_0^2-F_c^2)^2/\Sigma[\omega\ (F_0^2)^2]\}^{1/2}$.

Molecular Drawings
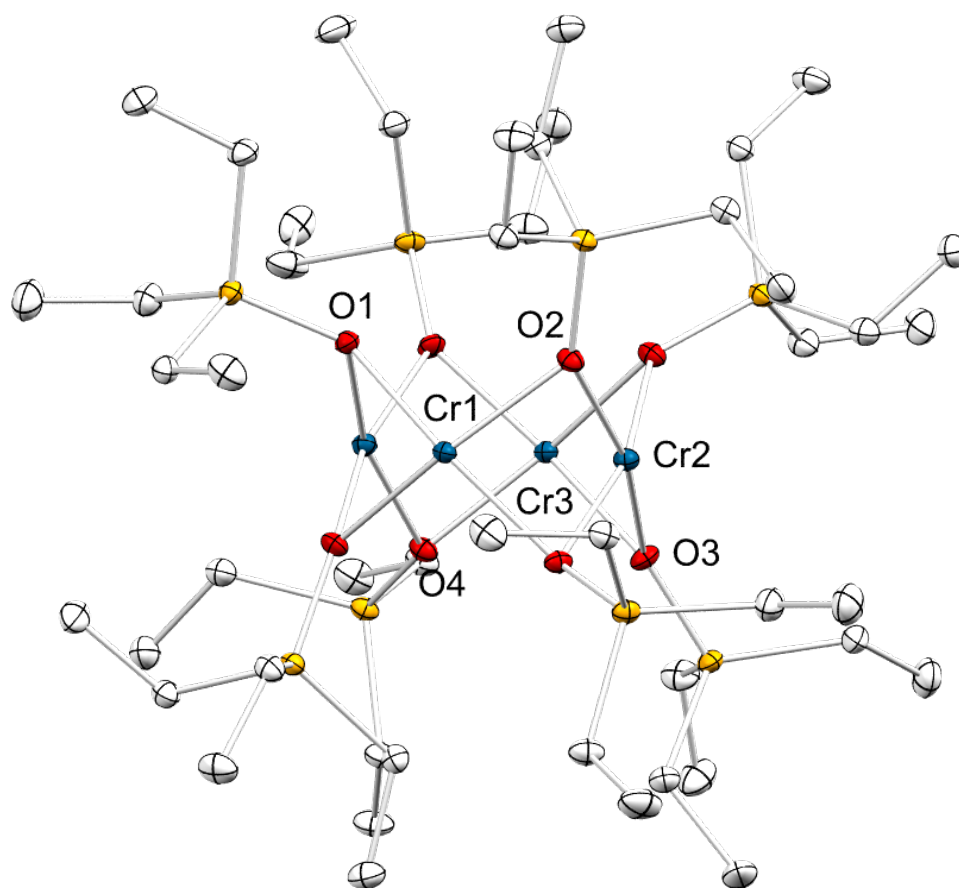
**Figure S22.** MERCURY representation (30% probability ellipsoids) of Cr$_4$(OSiEt$_3$)$_2$]$_8$ (**7**). Hydrogen atoms are omitted for clarity. Selected interatomic distances (Å) and angles (°): Cr1···Cr2 2.5381(6), Cr2···Cr3 2.5325(6), Cr1–O2 2.0046(17), Cr1–O1 2.0199(17), Cr2–O2 1.9907(17), Cr2–O3 1.9940(18), Cr3–O3 1.9939(17), Cr3–O4 2.0077(18), Si1–O1 1.6448(19), Si2–O2 1.6453(18), Si3–O3 1.6425(18), Si4–O4 1.6370(19); O2–Cr1–O1 98.30(7), O2–Cr1–Cr2 50.32(5), O1–Cr1–Cr2 114.93(5), Cr1–Cr2–Cr3 90.83(2), Cr(1)–O(1)–Si(1) 136.95(11), Cr(1)–O(2)–Si(2) 132.78(11), Cr(2)–O(2)–Si(2) 143.38(11), Cr(2)–O(3)–Si(3) 143.57(11), Cr(3)–O(3)–Si(3) 137.32(11), Cr(3)–O(4)–Si(4) 137.91(11).
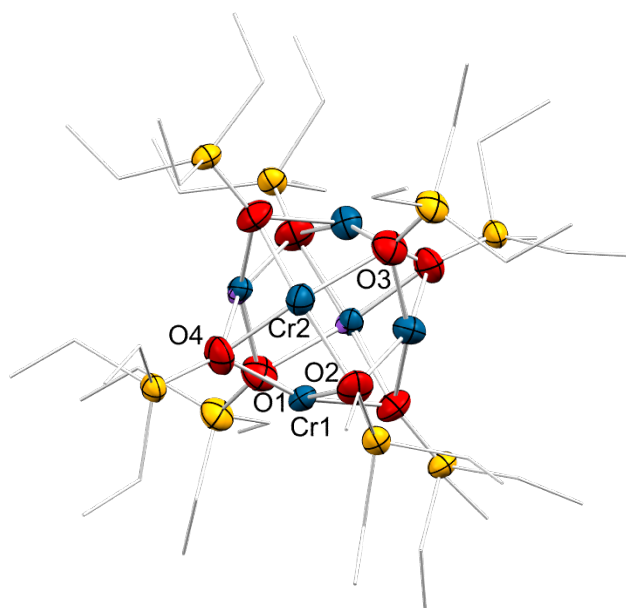
Figure S23. MERCURY representation (30% probability ellipsoids) of $Na_4Cr_2(OSiEt_3)_8$ (**8**). Hydrogen atoms are omitted for clarity Na1 and Na2 are completely covered by the ellipsoids of Cr1 and Cr2 and therefore not visible.
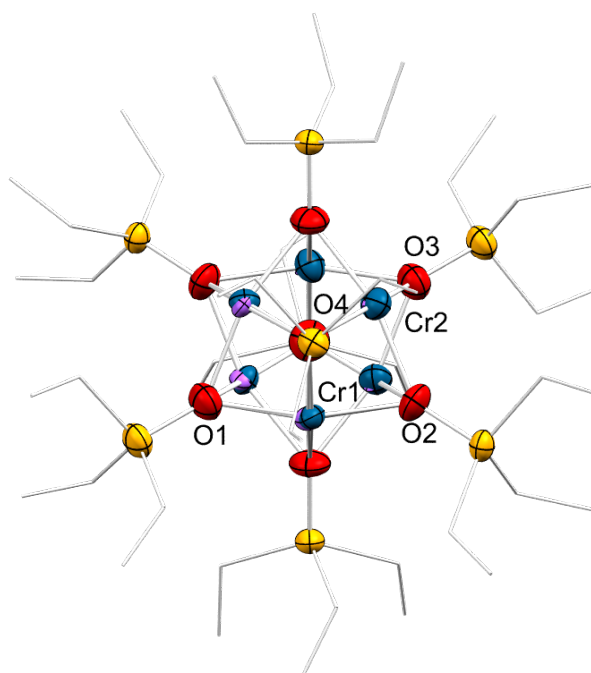

Figure S24. MERCURY representation (30% probability ellipsoids) of $Na_4Cr_2(OSiEt_3)_8$ (**8**). Hydrogen atoms are omitted for clarity.

The octahedron is built by Na and Cr. All six positions are partially occupied by Na and Cr. The disorder model should reveal a Na:Cr ratio of 2:1, to become at least a Na_4Cr_2 core. The refinement for the two positions in the asymmetric unit shows exact that ratio for one position, but for the second one we have a divergence (0.588:0.422). This result may be caused by the difficulties in structure solution and the overall disorder in the molecule. In the crystal, the "ball-like" cluster is orientated in distinct directions. Therefore, the averaged contents of the unit cell are obtained by averaging over the space, which leads to substitutional disorder. The divergence for the second position regarding the Na/Cr disorder might be also affect by partial hydrolysis as indicated by a significant OH stretching vibration in the IR spectrum (Figure S15).